Numerical study of a three-state host-parasite system on the square lattice

Takehisa Hasegawa[*]

Department of Mathematical Informatics, The University of Tokyo, 7-3-1 Hongo, Bunkyo, Tokyo 113-8656, Japan

Norio Konno[†]

Faculty of Engineering, Yokohama National University, 79-5 Tokiwadai, Hodogaya-ku, Yokohama, Japan

Naoki Masuda[‡]

Department of Mathematical Informatics, The University of Tokyo, 7-3-1 Hongo, Bunkyo, Tokyo 113-8656, Japan and
PRESTO, Japan Science and Technology Agency, 4-1-8 Honcho, Kawaguchi, Saitama 332-0012, Japan

We numerically study the phase diagram of a three-state host-parasite model on the square lattice motivated by population biology. The model is an extension of the contact process, and the three states correspond to an empty site, a host, and a parasite. We determine the phase diagram of the model by scaling analysis. In agreement with previous results, three phases are identified: the phase in which both hosts and parasites are extinct (S_0), the phase in which hosts survive but parasites are extinct (S_{01}), and the phase in which both hosts and parasites survive (S_{012}). We argue that both the S_0-S_{01} and $S_{01}-S_{012}$ boundaries belong to the directed percolation class. In this model, it has been suggested that an excessively large reproduction rate of parasites paradoxically extinguishes hosts and parasites and results in S_0. We show that this paradoxical extinction is a finite size effect; the corresponding parameter region is likely to disappear in the limit of infinite system size.

I. INTRODUCTION

In research fields ranging from ecology and epidemiology to sociology, it is important to clarify the effect of the interactions among species or phenotypes on the entire system. Stochastic interacting particle systems, in which each site on a graph takes either of the possible states and is flipped according to the states of other sites, are a useful tool for this purpose. A paradigmatic interacting particle system that describes disease spreading is the contact process (CP; also termed the susceptible-infected-susceptible model) [1–3].

Various interacting particle systems in complex networks have been investigated recently [4,5]. Nevertheless, in an ecological context, organisms of different scales can be considered to live in a two-dimensional space, often with a small interaction range. Therefore, it is instructive to study models that are more complex than the CP on the Euclidean lattice [3,6,7]. A simple extension of the CP in this direction is a three-state spatial host-parasite (HP) model that deals with an ecosystem comprising soil (empty sites), host species living on soil, and pathogen species (parasites) living on hosts. Phase transitions and oscillations in similar models have been studied from the perspective of statistical physics [8–12].

Satō *et al.* [13] analyzed the HP model on a square lattice. They showed by means of the improved-pair approximation (i-PA) and numerical simulations that a very high reproduction rate of parasites results in the extinction of both hosts and parasites. This phenomenon is called parasite-driven extinction [13,14]. An intuitive explanation for this paradoxical behavior is that parasites replace hosts so quickly that hosts get extinct, which eventually results in the extinction of parasites. A similar

paradoxical behavior (i.e., a decrease in the number of a species caused by an increase in its fertility) is observed in other models, where a sort of rock-scissors-paper competition is prevalent among three species [15–23]. However, the current understanding of the phase diagram of the HP model is not comprehensive because parasite-driven extinction cannot be predicted by mean-field approximation and pair approximation (PA) [24,25].

In this paper, we numerically investigate the phase diagram of the HP model on the square lattice. In particular, we use large lattices and investigate the effect of the system size on parasite-driven extinction. The obtained phase diagram is shown in Fig. 1. We argue that two transition boundaries (solid lines in Fig. 1) belong to the directed percolation (DP) universality class. Another transition boundary (dotted lines) is not characterized by the DP universality class, and its location depends on the system size. We claim that the parasite-driven extinction phase is a finite size effect and that the phase diagram is qualitatively the same as that obtained by the PA rather than that obtained by the i-PA.

II. MODEL

The HP model on the square lattice $\mathbb{Z}^2$ is defined as a continuous-time Markov process with state space $\{0,1,2\}^{\mathbb{Z}^2}$ [13,14,24–26]. Each site takes one of the three states $0,1$, and 2, which represent an empty site, a host, and a parasite, respectively. The rules for the state transition are depicted in Fig. 2. A host and a parasite die at rates d_1 and d_2, respectively. For simplicity, we set $d_1 = d_2 = 1$. The occurrence of death at any site is independent of the states of the neighboring sites. In contrast, reproduction of hosts and parasites depends on the states of the neighbors. A host emerges at an empty site i at rate $\lambda_{01} n_1(i)$, where $n_1(i)$ is the number of hosts in the neighborhood of site i. A host at site i turns into a parasite at

————
[*]hasegawa@stat.t.u-tokyo.ac.jp
[†]konno@ynu.ac.jp
[‡]masuda@mist.i.u-tokyo.ac.jp
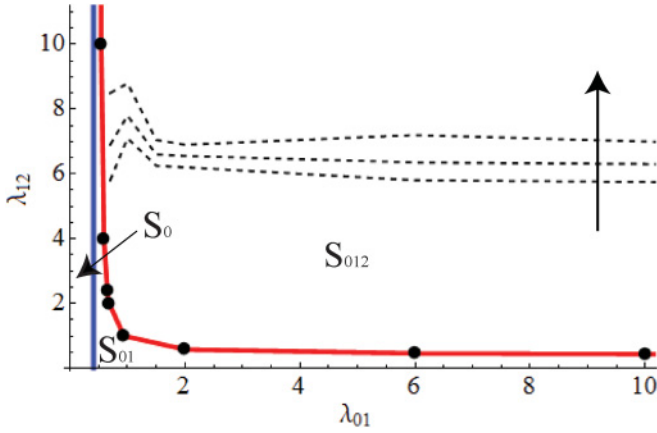
FIG. 1. (Color online) Phase diagram of the HP model. The solid blue line represents the boundary between S_0 and S_{01} (i.e., $\lambda_{01} = \lambda_{01}^c$). The solid red line represents the boundary between S_{01} and S_{012} and is drawn on the basis of the data shown in Table I. Above the dashed lines, which correspond to $L = 300, 500$, and 1000 from the bottom to the top, the parasite-driven extinction occurs frequently.

rate $\lambda_{12} n_2(i)$, where $n_2(i)$ denotes the number of parasites in the neighborhood of site i. We vary the values of λ_{01} and λ_{12} in the numerical simulations. Because parasites feed on hosts, the HP model allows the following three phases in the stationary state: (i) phase S_0, in which hosts and parasites are extinct; (ii) phase S_{01}, in which hosts survive and parasites are extinct; and (iii) phase S_{012}, in which both hosts and parasites survive.

The HP model with $\lambda_{12} = 0$ is equivalent to the CP. In the CP, each site takes either state 0 or 1, and a death event $(1 \rightarrow 0)$ and a reproduction event $(0 \rightarrow 1)$ at site i occur at rate $d_1 = 1$ and $\lambda_{01} n_1(i)$, respectively. In the case of the CP on the square lattice, S_0 and S_{01} are realized when λ_{01} is, respectively, smaller and larger than $\lambda_{01}^c \approx 0.4122$ [1].

The phase diagram of the HP model on the square lattice has been examined using the mean-field approximation [13]; the PA, which accounts for pairwise state correlation [24]; and the i-PA, which calibrates the PA to account for the aggregation of the same species in the space [13,14]. All of the three approximations predict the existence of the three phases of the model. In the mean-field approximation and the PA, the system is in S_0 if λ_{01} is less than a critical value that is independent of λ_{12}. Otherwise, the system is in S_{01} (S_{012}) when the value

of λ_{01} and λ_{12} is sufficiently small (large). In the mean-field approximation and the PA, the boundary between S_{01} and S_{012} is given by $\lambda_{12} = \lambda_{01}/(4\lambda_{01} - 1)$ and $\lambda_{12} = (12(\lambda_{01})^2 + 4\lambda_{01})/(36(\lambda_{01})^2 - 4\lambda_{01} - 3)$, respectively [24]. In particular, only S_0 and S_{012} exists when $\lambda_{12} \rightarrow \infty$ in the mean-field approximation. In the PA, when $\lambda_{12} \rightarrow \infty$, S_0, S_{01}, and S_{012} appear in this order in the PA as λ_{01} increases. The phase diagram obtained from the i-PA is qualitatively distinct from those obtained from the mean-field approximation and the PA. When λ_{12} is large, the i-PA predicts S_0 regardless of the value of λ_{01}. This result corresponds to the numerical observation that a large reproduction rate of parasites induces extinction of hosts and parasites [13,14]. We call this phenomenon the parasite-driven extinction. The mean-field approximation and the PA do not predict the existence of the parasite-driven extinction.

III. DP TRANSITION ON THE $S_{01}-S_{012}$ BOUNDARY FOR SMALL λ_{12}

In this section, we numerically examine the boundary between S_{01} and S_{012} for small values of λ_{12} (the red solid line in Fig. 1). We carry out Monte Carlo simulations for the HP model on the square lattice with $N = L \times L$ sites, where $L = 300$. Periodic boundary conditions are assumed. We run 500 realizations for fixed λ_{01} and λ_{12}. At the beginning of each realization, each site independently takes state 0, 1, or 2 with equal probability. We adopt an event-driven update algorithm in which we select one out of all the possible events to occur with the appropriate probability for each time step. Then, we increment the time by an appropriate amount.

First, we focus on the limit $\lambda_{01} \rightarrow \infty$, where an empty site adjacent to a host is instantaneously replaced by the host. A cluster of empty sites survives only when they are surrounded by a shell of parasites. When λ_{12} is small, parasites rarely form such a shell. Then, the HP model behaves like the CP, where empty sites and hosts in the HP model collectively correspond to the susceptible sites (i.e., state 0) in the CP. Because many spatial stochastic processes including the CP undergo a DP-type phase transition [1,27–29], we expect that the HP model also undergoes a DP-type transition from S_{01} to S_{012} as λ_{12} is increased to cross $\approx \lambda_{01}^c \approx 0.4122$. The time courses of the mean density of parasites $\langle \rho_2 \rangle(t)$ are shown in Fig. 3(a) for various values of λ_{12}, where $\langle \cdot \rangle$ denotes the average over all the realizations. At $\lambda_{12} = \lambda_{12}^c \approx 0.4129$, we obtain

$$\langle \rho_2 \rangle(t) \propto t^{-\delta}. \tag{1}$$

From Fig. 3(b), which shows the plotting of the local slopes of $\langle \rho_2 \rangle(t)$, we obtain $\delta \approx \log\langle \rho_2 \rangle(t)/\log t \approx 0.451$, a value indicative of the DP universality class [1]. We also derive δ via dynamic scaling [27,28], that is, by fitting the following scaling form:

$$\langle \rho_2 \rangle(t) \approx t^{-\beta/\nu_\parallel} \tilde{\rho}_2 \left(\Delta\lambda_{12} t^{1/\nu_\parallel}, \frac{t^{d/z}}{N} \right), \tag{2}$$

where

$$\Delta\lambda_{12} = \lambda_{12} - \lambda_{12}^c. \tag{3}$$

The critical exponent δ is given by $\delta = \beta/\nu_\parallel$. The results of the dynamic scaling with the known critical exponents for

FIG. 2. Transition rules of the HP model. Solid and dashed lines represent deaths and births, respectively. The values indicate the transmission rates, and n_i denotes the number of neighbors of a site in state i.
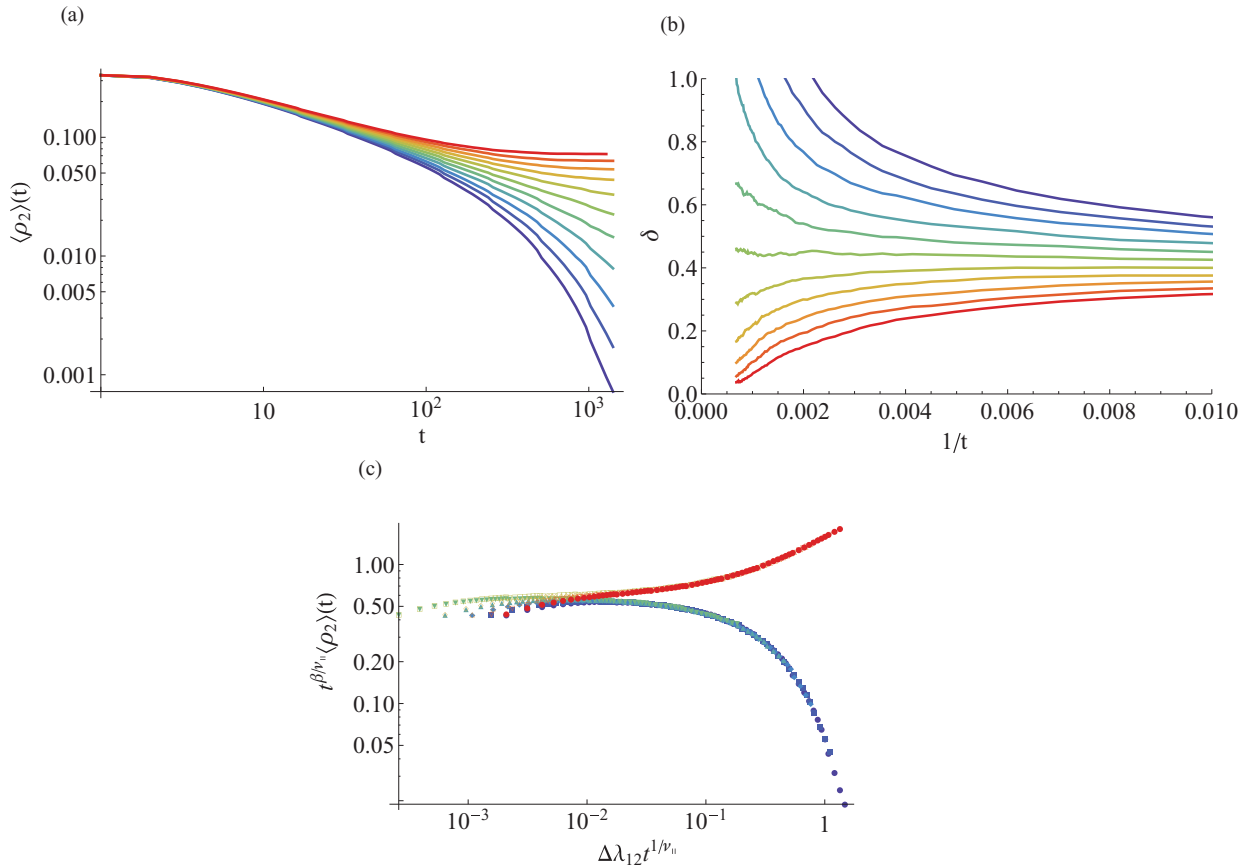
FIG. 3. (Color online) DP phase transition at $\lambda_{01} \to \infty$ and $\lambda_{12} \approx \lambda_{12}^c$. (a) Time courses of $\langle \rho_2 \rangle(t)$ and (b) local slope δ of $\langle \rho_2 \rangle(t)$. The different lines from the top to the bottom correspond to $\lambda_{12} = 0.4079, 0.4089, \ldots,$ and 0.4179. (c) Dynamic scaling [Eq. (2)] for the data shown in (b).

the $(2+1)$-dimensional DP universality class $\beta \approx 0.583$ and $\nu_{\parallel} \approx 1.295$ [1] are shown in Fig. 3(c). The data for different values of λ_{12} collapse onto a single curve separately for subthreshold and suprathreshold values of λ_{12}. This result also supports that the transition belongs to the DP universality class.

If λ_{01} is finite and sufficiently large, we can numerically obtain the transition points and the critical exponents in the

same manner. On the critical line, $\langle \rho_2 \rangle(t)$ shows a power-law decay with t, as shown in Fig. 4(a). When $\lambda_{01} \gtrsim 0.68$, the dynamic scaling yields the DP critical exponents at each examined transition point. The locations of several points on the S_{01}–S_{012} boundary are shown in Fig. 1 and Table I.

We postpone the analysis of the case $\lambda_{01} \lesssim 0.68$ to Sec. VI.
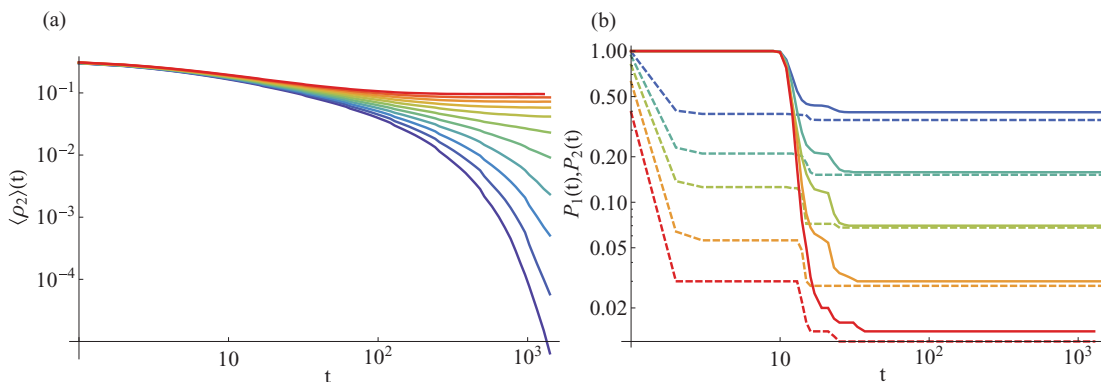
FIG. 4. (Color online) (a) Time courses of $\langle \rho_2 \rangle(t)$ with $\lambda_{01} = 10$. The lines from the top to the bottom correspond to $\lambda_{12} = 0.430, 0.432, \ldots,$ and 0.450. (b) Surviving probability of hosts $P_1(t)$ (dashed lines) and that of parasites $P_2(t)$ (solid lines) with $\lambda_{01} = 10$. The lines from the top to the bottom correspond to $\lambda_{12} = 5.9, 6.3, 6.7, 7.1,$ and 7.5. We set $L = 300$ in both (a) and (b).

TABLE I. Several points on the $S_{01}-S_{012}$ boundary.

λ_{01}	0.509	0.543	0.591	0.651	0.680	0.942	2.000	6.000	10.000	15.000	20.000	∞
λ_{12}	∞	10.000	4.000	2.378	2.000	1.000	0.581	0.459	0.440	0.430	0.426	0.4129

IV. DEPENDENCE OF BOUNDARY BETWEEN S_{012} AND THE PARASITE-DRIVEN EXTINCTION REGION ON λ_{12}

Parasite-driven extinction may occur for large λ_{12} [13,14]. Figure 4(b) shows the surviving probability of hosts $P_1(t)$ and that of parasites $P_2(t)$ for some large values of λ_{12} and fixed values of $\lambda_{01} = 10$ and $L = 300$. If $P_1(t)$ approaches zero rapidly, the parasite-driven extinction is considered to have occurred. If the transition from S_{012} to the parasite-driven extinction belongs to the DP universality class, $P_1(t)$ or $P_2(t)$ should decay geometrically on the phase boundary and exponentially for λ_{12} slightly larger than the critical value.

However, Fig. 4(b) indicates that this is not the case. Whether extinction of hosts and parasites occurs or not is determined at an early stage, where hosts are rapidly replaced by parasites, resulting in a rapid decrease in the number of hosts. If the hosts die out, the parasite-driven extinction takes place. In contrast, if hosts survive the initial stage, which occurs with a low probability, the hosts recover from near extinction. In this case, hosts and parasites are likely to coexist for a long time. The value of λ_{12} affects the probability that the hosts survive rather than the rates at which the number of hosts and parasites decay.

We state that the parasite-driven extinction is a finite size effect. To confirm this statement, we measure the probability of the parasite-driven extinction as a function of linear lattice size L. Because the transient is short, as shown in Fig. 4(b), we measure the fraction of realizations among 2000 realizations in which both hosts and parasites are extinct at $t = 100$. Figure 5(a) shows the extinction probability for a range of values of λ_{12} at $\lambda_{01} = 10$ and $L = 100, 200, 300, 500, 700$, and 1000. The extinction probability indefinitely decreases with L. The value of λ_{12} that has an extinction probability of 1/2, denoted by $\lambda_{12} = \lambda_{12}^f(\lambda_{01}, L)$, is plotted against L in

Fig. 5(b). It is observed that $\lambda_{12}^f(\lambda_{01}, L) \propto \ln L$. Logarithmic scaling is also observed at other values of λ_{01}. In Fig. 1, we show $\lambda_{12}^f(\lambda_{01}, L)$ for some values of λ_{01} and L (dotted lines).

The results obtained in this section indicate that the parameter region of parasite-driven extinction indefinitely shrinks as L increases. This system-size dependence is distinct from the dependence of the critical value on L in the usual phase transitions, which is convergent in the limit of infinite system size.

V. DP TRANSITION ON THE S_0-S_{01} BOUNDARY IN THE LIMIT $\lambda_{12} \to \infty$

When λ_{12} is sufficiently large, the mean-field approximation predicts that the system transits from S_0 to S_{012} as λ_{01} increases [13]. The PA predicts that the system transits from S_0 to S_{01} and then to S_{012} as λ_{01} increases [24]. The i-PA predicts that the system is in S_0 irrespective of the value of λ_{01} (see Fig. 1 in Ref. [14]). To analyze this apparent contradiction, we carry out simulations in the limit $\lambda_{12} \to \infty$.

Irrespective of the value of λ_{12}, it seems that λ_{01} must be larger than λ_{01}^c for hosts to survive. Therefore, we start by examining the case $\lambda_{01} \approx \lambda_{01}^c$. When $\lambda_{01} \approx \lambda_{01}^c$ and $\lambda_{12} \to \infty$, a host adjacent to a parasite is instantaneously invaded by the parasite. In such a case, if we start numerical simulations on the equal fraction of empty sites, hosts, and parasites, then the number of hosts, if they survive at all, becomes small at the very beginning of a run. For example, the averaged number of hosts on the 300×300 square lattice decreases from 30 000 to ≈ 60 after a short time. It may not be suitable to measure the decay of the expected number of hosts, which would be $\langle \rho_1 \rangle(t) \propto t^{-\delta}$ on the critical line; this is because such a measurement necessitates the existence of a sufficiently large number of hosts at the beginning of a run.

Another numerical method for estimating the transition point and critical exponents is to measure the time courses
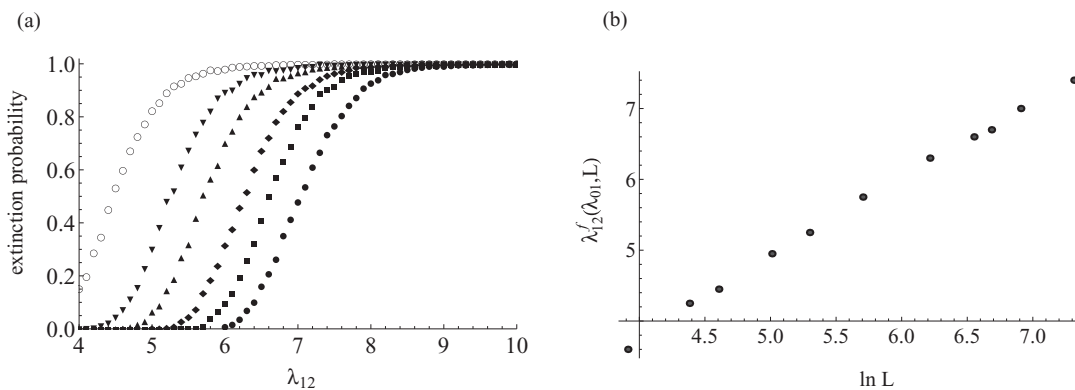
FIG. 5. (a) Relationship between the extinction probability and λ_{12} when $L = 100, 200, 300, 500, 700$, and 1000 (from left to right). (b) Dependence of $\lambda_{12}^f(\lambda_{01}, L)$ on L. We set $\lambda_{01} = 10$ in both (a) and (b). The number of realizations for a given combination of λ_{12} and L is equal to 2000.
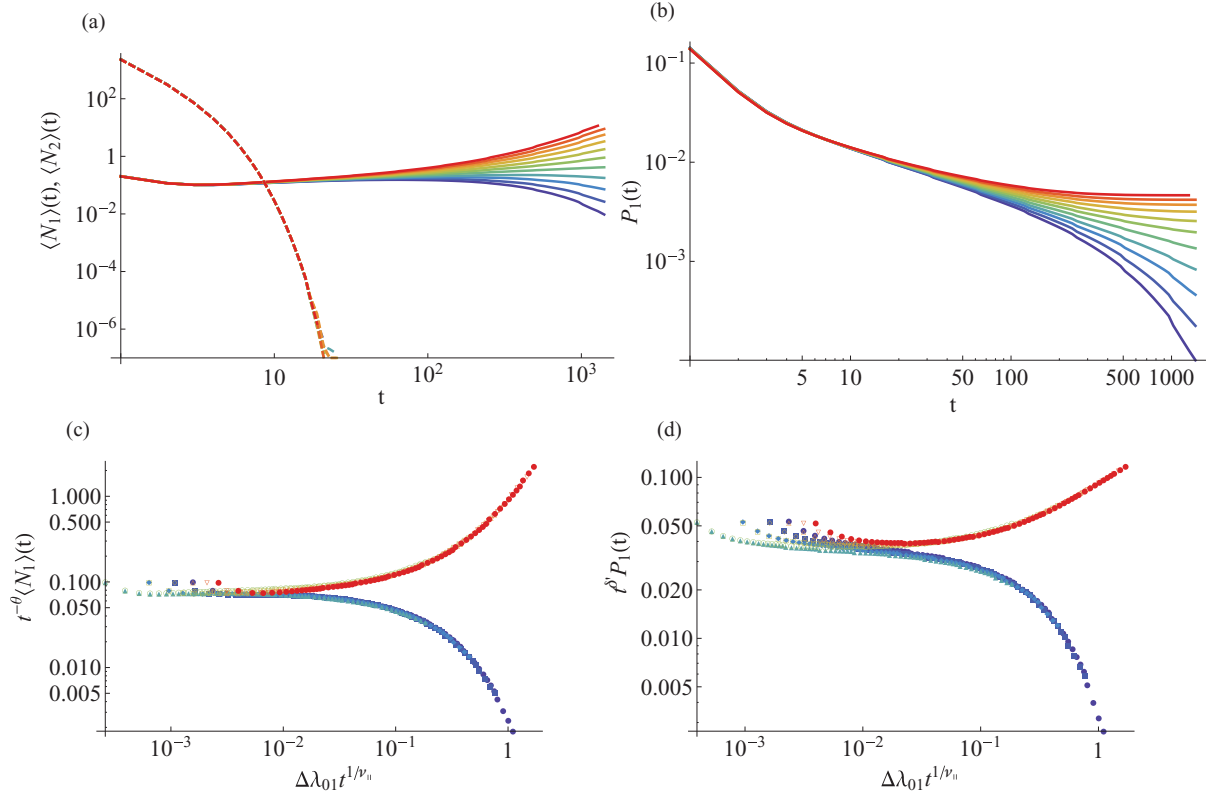
FIG. 6. (Color online) Transitions at $\lambda_{01} \approx \lambda_{01}^c$ and $\lambda_{12} \to \infty$. (a) Time courses of $\langle N_1 \rangle(t)$ (solid lines) and $\langle N_2 \rangle(t)$ (dashed lines that almost overlap each other). (b) Surviving probability of hosts $P_1(t)$. (c) Dynamic scaling [Eq. (4)] for the data shown in (a). (d) Dynamic scaling [Eq. (5)] for the data shown in (b). The lines correspond to $\lambda_{01} = 0.4082, 0.4092, \dots$, and 0.4182 from the bottom to the top. The number of realizations for a given λ_{01} is equal to 10^7.

of the system starting from an almost absorbing configuration [30]. For example, we observe the power-law behavior of the surviving probability, the number of active sites, and the mean spreading at the transition point, if we run the CP starting from a single active site. Therefore, we assume that the initial configuration of the HP model contains just one host. The other sites are either empty or parasites with a probability of 0.5.

With this one-host configuration, the mean number of hosts follows the power law $\langle N_1 \rangle(t) \propto t^\theta$ at $\lambda_{01} \approx \lambda_{01}^c$, as shown by the solid lines in Fig. 6(a). On the other hand, parasites rapidly become extinct (dashed line). The surviving probability of hosts also follows the approximate power law $P_1(t) \propto t^{-\delta'}$ in the same parameter range [Fig. 6(b)].

At $\lambda_{01} \approx \lambda_{01}^c$, we adopt the dynamic scaling ansatz [1] represented by

$$\langle N_1 \rangle(t) \approx t^\theta \tilde{N}_1 \left(\Delta\lambda_{01} t^{1/\nu_\parallel}, \frac{t^{d/z}}{N} \right), \qquad (4)$$

$$P_1(t) \approx t^{-\delta'} \tilde{P}_1 \left(\Delta\lambda_{01} t^{1/\nu_\parallel}, \frac{t^{d/z}}{N} \right), \qquad (5)$$

where

$$\Delta\lambda_{01} = \lambda_{01} - \lambda_{01}^c. \qquad (6)$$

This dynamic scaling ansatz explains the data shown in Figs. 6(a) and 6(b), respectively. The fitting results with the DP exponents $\theta \approx 0.229$ and $\delta' = \delta \approx 0.451$ [1] [Figs. 6(c) and 6(d)] suggest that the transition from S_0 to S_{01} at $\lambda_{01} = \lambda_{01}^c$

and $\lambda_{12} \to \infty$ is of the DP type. We consider that this phase transition is independent of the value of λ_{12}. This result qualitatively agrees with that obtained from the PA but not that obtained from the i-PA.

With the random initial configuration, we observe $\langle N_1 \rangle(t)$ and $P_1(t)$ instead of $\langle \rho_1 \rangle(t)$ and obtain the same results as those shown in Fig. 6. $\langle N_1 \rangle(t)$ and $P_1(t)$ decay geometrically at $\lambda_{01} \approx \lambda_{01}^c$, as shown in Figs. 7(a) and 7(b), respectively. The dynamic scaling [Eq. (4)] with the DP exponents fits $\langle N_1 \rangle(t)$ shown in Fig. 7(a) well [Fig. 7(c)]. On the other hand, dynamic scaling of $P_1(t)$ [Eq. (5)] fails because the number of surviving hosts after a short time is greater than one. To circumvent this case, we assume that the surviving hosts are located away from each other and grow independently on the lattice. We denote the surviving probability of a specified host by $P_1^{\text{single}}(t)$. Then, we approximate $P_1(t)$ as

$$P_1(t) \approx 1 - \left[1 - P_1^{\text{single}}(t) \right]^n, \qquad (7)$$

that is,

$$P_1^{\text{single}}(t) \approx 1 - [1 - P_1(t)]^{1/n}, \qquad (8)$$

where n is the mean number of surviving hosts after a short time. By replacing $P_1(t)$ in Eq. (5) by $P_1^{\text{single}}(t)$ and using the DP critical exponents, we obtain a reasonable scaling, as shown in Fig. 7(d).
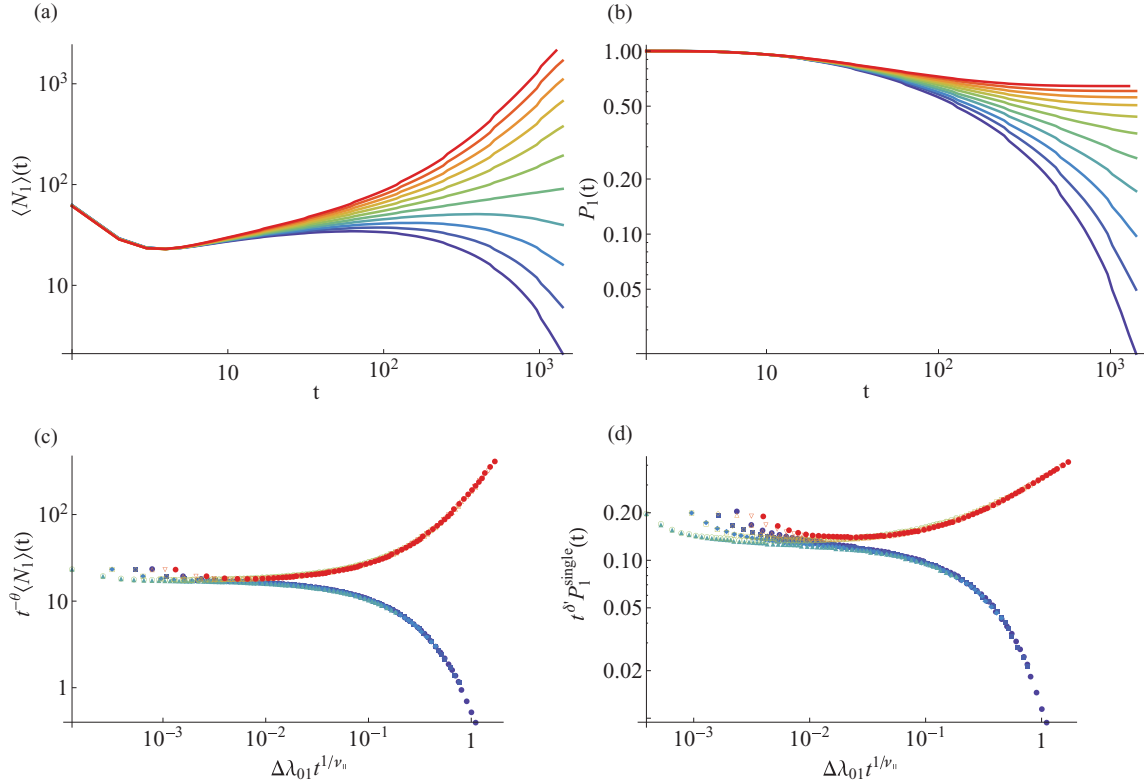
FIG. 7. (Color online) (a) Time courses of $\langle N_1 \rangle(t)$ when $\lambda_{01} \approx \lambda_{01}^c$. (b) Surviving probability of hosts $P_1(t)$. (c) Dynamic scaling [Eq. (4)] for the data shown in (a). (d) Dynamic scaling with Eqs. (5) and (8) applied to the data shown in (b). The lines correspond to $\lambda_{01} = 0.40821, 0.40921, \ldots$, and 0.41821 from the bottom to the top. The number of realizations for a given λ_{01} is equal to 10^7.

VI. S_{012} PHASE IN THE LIMIT $\lambda_{12} \to \infty$

When $\lambda_{12} \to \infty$, either the random initial configuration or the one-host configuration yields S_0 or S_{01}, but not S_{012}, for any value of λ_{01}. This remains the case for at least up to $L = 1000$. The apparent absence of S_{012} may be because there are initially too many parasites. In the case of a large λ_{12}, parasites replace hosts in a short time, which is likely to lead to the extinction of the parasite.

To examine the possibility of S_{012} at $\lambda_{12} \to \infty$, we adopt the one-parasite configuration, where the remaining sites are either empty or occupied by the host with a probability of 0.5. With this initial configuration, we find that both hosts and parasites can survive when L is large and λ_{01} is within a certain range. When $L \lesssim 400$, neither hosts nor parasites survive.

Time courses of the number of parasites are shown in Fig. 8 for $L = 700$ and three values of λ_{01}. As λ_{01} increases within this range, the basal number of parasites in a short run increases, but the amplitude of the damped oscillation in the number of parasites also increases. If λ_{01} is sufficiently large, the amplitude of the oscillation is so large that the parasites are likely to disappear in the first cycle of the oscillation [Fig. 8(c)], whereas the basal number of parasites is larger than that in the case of a smaller λ_{01} [e.g., Fig. 8(a)]. We remark that, for related spatial stochastic processes, sustainable oscillations [31, 32] and absorption to the unanimity state owing to the blowing out of oscillations [33] were reported as finite size effects.

The stationary density of the parasites averaged over the surviving runs, denoted by $\langle \rho_2 \rangle_{surv}$, is shown for some large

values of L in Fig. 9(a). Here $\langle . \rangle_{surv}$ indicates the average over realizations in which parasites survive after a transient of length 1500. We observe that $\langle \rho_2 \rangle_{surv}$ is positive for $\lambda_{01} \gtrsim 0.509$ and converges to a certain value for $\lambda_{01} \gtrsim 0.518$. We did not determine the transition point and the critical exponents by a scaling argument for $\langle \rho_2 \rangle_{surv}$ in terms of λ_{01} because $\langle \rho_2 \rangle_{surv}$ is too small for $\lambda_{01} \approx 0.509$. To support the existence of the S_{012} phase in the limit $L \to \infty$, we measure the fraction of surviving runs for various system sizes. As shown in Fig. 9(b), the fraction of surviving runs increases with L for $\lambda_{01} \gtrsim 0.509$. This result supports the fact that S_{012} exists for $\lambda_{01} \gtrsim 0.509$ in the limit $L \to \infty$. As λ_{01} increases even further (i.e., $\lambda_{01} \gtrsim 0.524$), the fraction of surviving runs decreases. The parasite-driven extinction for a finite system size gets eminent in this range of λ_{01}; this parasite-driven extinction is caused by the increasing magnitude of damped oscillations. Similar to the results shown in Sec. IV, the parameter region for the parasite-driven extinction depends on the system size and is likely to disappear in the limit $L \to \infty$. We also observed that the results in the case of finite $\lambda_{12} \gtrsim 2$ are qualitatively the same as those in the case of $\lambda_{12} = \infty$.

Finally, we examine the S_{01}–S_{012} transition line for large λ_{12}. In this case, we do not obtain a data collapse by the dynamic scaling based on the relaxation of the system, as shown in Fig. 10(a) for $\lambda_{12} = 4$. Therefore, we attempt the dynamic scaling for the parasites in the manner similar to that employed in Sec. V. Consider the neighborhood of the S_{01}–S_{012} transition point for a large fixed λ_{12}. With the one-parasite configuration, a parasite would quickly invade hosts at an early
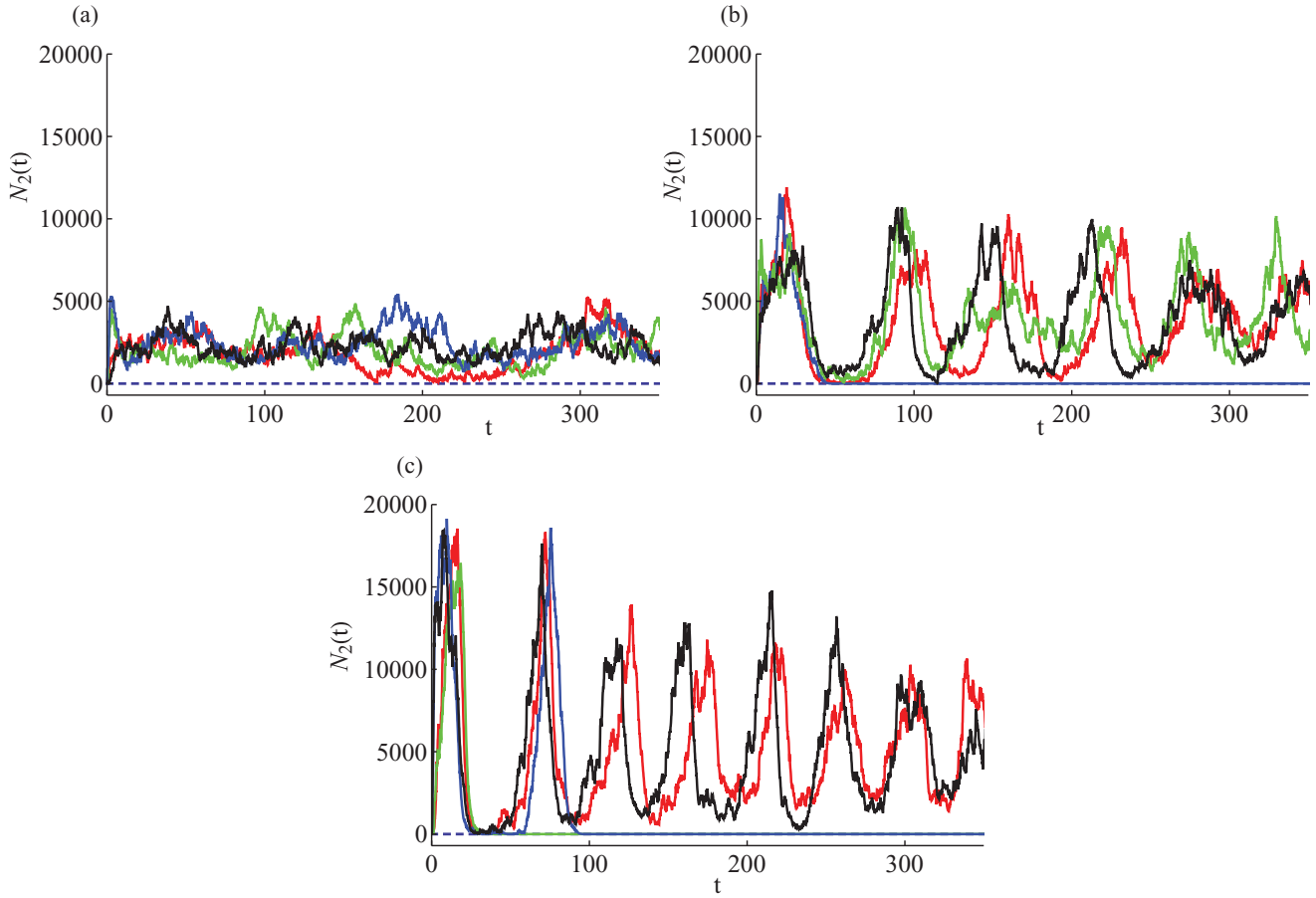
FIG. 8. (Color online) Time courses of $N_2(t)$ when $\lambda_{01} =$ (a) 0.515, (b) 0.530, and (c) 0.545. We set $\lambda_{12} \to \infty$ and $L = 700$. Each colored line represents a single run, and the results for four runs are shown in each panel.

stage. In this case, the growth rate of the parasite is fairly insensitive to λ_{01}. Therefore, the scaling argument would not apply.

To avoid such an initial growth of parasites and obtain a clear scaling of $\langle N_2 \rangle(t)$, we proceed as follows. First, we start a simulation from a mixture of independently distributed empty sites and hosts with the equal density (i.e., 0.5 each). After the system has approached a steady S_{01} state, we replace

a randomly chosen empty site with a parasite and continue the simulation until the stationary state is reached. Figure 10(b) shows the time course of $\langle N_2 \rangle(t)$ for $\lambda_{12} = 4$ and various values of λ_{01}, where the single parasite is added at $t = 0$. Near the transition point, $\lambda_{01} \sim 0.591$, $\langle N_2 \rangle(t)$ seems to follow a power law. The data for different values of λ_{12} collapse onto a single curve with the DP critical exponents, separately for subthreshold and suprathreshold values of λ_{01} [Fig. 10(c)].
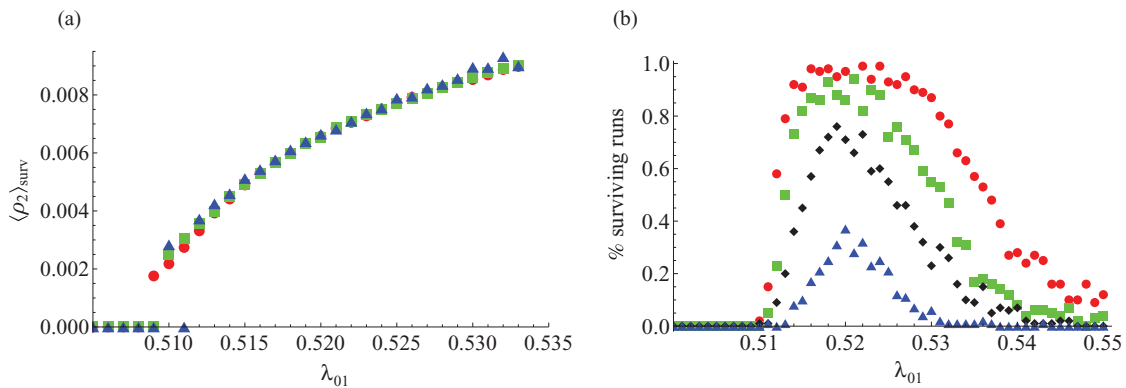
FIG. 9. (Color online) (a) Stationary parasite density $\langle \rho_2 \rangle_{\text{surv}}$ averaged over the surviving runs in the limit $\lambda_{12} \to \infty$. (b) Fraction of the surviving runs. We set $L = 500$ (triangles), 600 [diamonds; only in (b)], 700 (squares), and 900 (circles). The number of realizations for a given combination of λ_{01} and L is equal to 100.
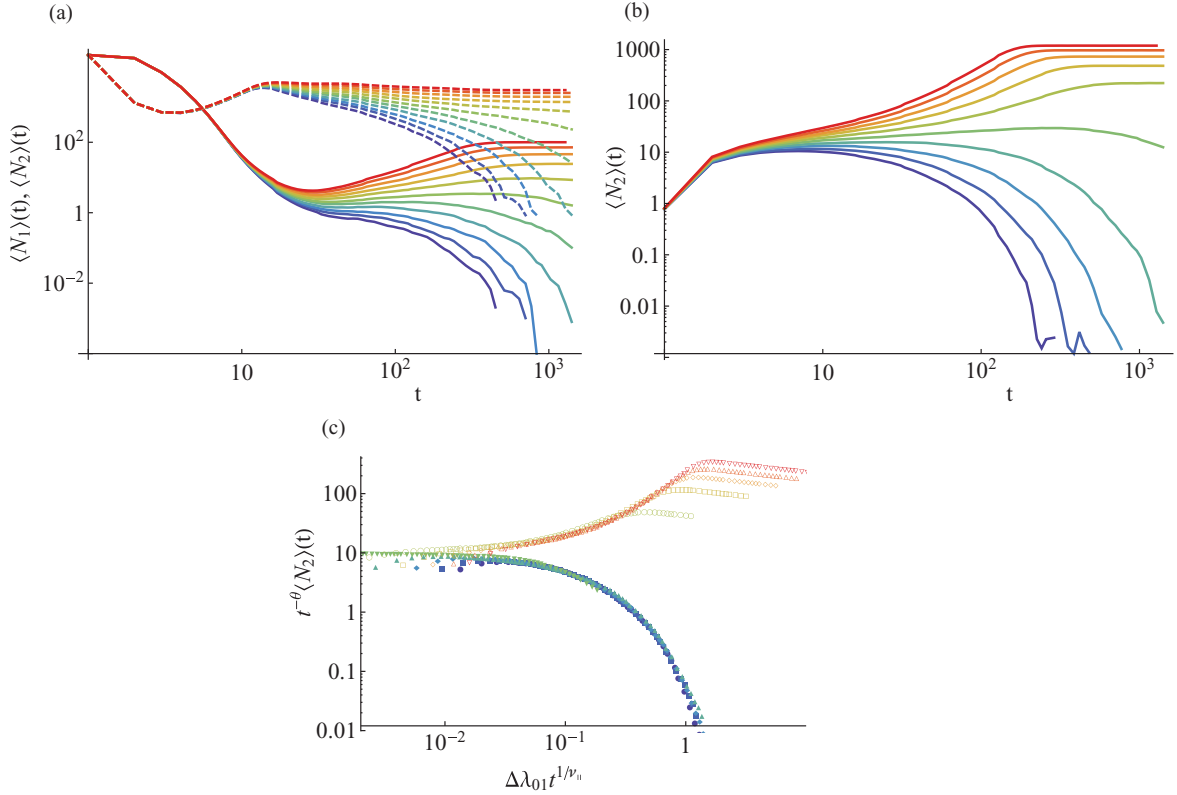
FIG. 10. (Color online) (a) Time courses of $\langle N_1 \rangle(t)$ (dashed lines) and $\langle N_2 \rangle(t)$ (solid lines) for the random initial configuration. The lines from the bottom to the top correspond to $\lambda_{01} = 0.58, 0.582, \ldots$, and 0.60. The number of realizations for a given λ_{01} is equal to 50 000. (b) Time courses of $\langle N_2 \rangle(t)$ for the modified initial configuration. The lines correspond to $\lambda_{01} = 0.57, 0.575, \ldots$, and 0.615 from the bottom to the top. The number of realizations for a given λ_{01} is equal to 20 000. We set $\lambda_{12} = 4$ and $L = 300$ in both (a) and (b). (c) Dynamic scaling for the data shown in (b). As the scaling function, we use Eq. (4) with $\langle N_1 \rangle(t)$ replaced by $\langle N_2 \rangle(t)$.

Figure 10(c) suggests that the transition belongs to the DP universality class.

Note that $\langle N_2 \rangle(t)$ above the transition point saturates owing to a finite size effect. It is difficult to determine critical properties for large values of λ_{12} because we would need increase L to perform the dynamic scaling. Nevertheless, we believe that the $S_{01}-S_{012}$ transition belongs to the DP universality class even for larger λ_{12}.

VII. SUMMARY

We carried out numerical simulations for a three-state host-parasite model on the square lattice. The obtained phase diagram is shown in Fig. 1. Our numerical results suggest that the S_0-S_{01} boundary and the $S_{01}-S_{012}$ boundary are of the DP universality class. The parasite-driven extinction occurs for large λ_{01} and large λ_{12} in relatively small systems. However,

for a sufficiently large system, the three states coexist in the parameter region where the parasite-driven extinction occurs for a small system. Therefore, the parasite-driven extinction is a finite size effect. This prediction is consistent with the phase diagram obtained from the PA but not with phase diagrams obtained from the mean field approximation and the i-PA.

ACKNOWLEDGMENTS

[1] J. Marro and R. Dickman, *Nonequilibrium Phase Transitions in Lattice Models* (Cambridge University Press, Cambridge, England, 1999).

[2] T. M. Liggett, *Interacting Particle Systems* (Springer-Verlag, New York, 1985).

[3] R. Durrett and S. A. Levin, Philos. Trans. R. Soc. London B **343**, 329 (1994).

[4] M. E. J. Newman, SIAM Rev. **45**, 167 (2003).

[5] A. Barrat, M. Barthélemy, and A. Vespignani, *Dynamical Processes on Complex Networks* (Cambridge University Press, Cambridge, England, 2008).

[6] U. Dieckmann, R. Law, and J. A. J. Metz, *The Geometry of Ecological Interactions: Simplifying Spatial Complexity* (Cambridge University Press, Cambridge, England, 2000).

[7] R. M. Anderson and R. M. May, *Infectious Diseases of Humans* (Oxford University Press, New York, 1991).

[8] T. Antal, M. Droz, A. Lipowski, and G. Ódor, Phys. Rev. E **64**, 036118 (2001).

[9] T. Antal and M. Droz, Phys. Rev. E **63**, 056119 (2001).

[10] K. C. de Carvalho and T. Tomé, Mod. Phys. Lett. B **18**, 873 (2004).

[11] K. C. de Carvalho and T. Tomé, Int. J. Mod. Phys. C **17**, 1647 (2006).

[12] M. Peltomäki, V. Vuorinen, M. Alava, and M. Rost, Phys. Rev. E **72**, 046134 (2005).

[13] K. Satō, H. Matsuda, and A. Sasaki, J. Math. Biol. **32**, 251 (1994).

[14] Y. Haraguchi and A. Sasaki, J. Theor. Biol. **203**, 85 (2000).

[15] M. Boots and A. Sasaki, Ecol. Lett. **3**, 181 (2000).

[16] M. Boots and A. Sasaki, Amer. Nat. **159**, 706 (2002).

[17] M. Boots and A. Sasaki, Ecol. Lett. **6**, 176 (2003).

[18] K. Tainaka, Phys. Lett. A **176**, 303 (1993).

[19] K. Tainaka, Phys. Lett. A **207**, 53 (1995).

[20] M. Frean and E. R. Abraham, Proc. R. Soc. London B **268**, 1323 (2001).

[21] J. J. Ryder, M. R. Miller, A. White, R. J. Knell, and M. Boots, Oikos **116**, 2017 (2007).

[22] A. Lipowski, Phys. Rev. E **60**, 5179 (1999).

[23] M. Kowalik, A. Lipowski, and A. L. Ferreira, Phys. Rev. E **66**, 066107 (2002).

[24] K. Ohtsuka, N. Konno, N. Masuda, and K. Aihara, Int. J. Bifurcation Chaos Appl. Sci. Eng. **16**, 3687 (2006).

[25] K. Satō and N. Konno, J. Phys. Soc. Jpn. **64**, 1866 (1995).

[26] E. Andjel and R. Schinazi, J. Appl. Probab. **33**, 741 (1996).

[27] H. Hinrichsen, Physica A **369**, 1 (2006).

[28] H. Hinrichsen, Adv. Phys. **49**, 815 (2000).

[29] G. Ódor, Rev. Mod. Phys. **76**, 663 (2004).

[30] P. Grassberger and A. de la Torre, Ann. Phys. (NY) **122**, 373 (1979).

[31] Y. Itoh and K. Tainaka, Phys. Lett. A **189**, 37 (1994).

[32] S. Morita and K. Tainaka, Popul. Ecol. **48**, 99 (2006).

[33] G. Szabó, A. Szolnoki, and R. Izsák, J. Phys. A: Math. Theor. **37**, 2599 (2004).